ACS APPLIED MATERIALS & INTERFACES

Research Article

www.acsami.org

PLGA-Mesoporous Silicon Microspheres for the *in Vivo* Controlled Temporospatial Delivery of Proteins

Silvia Minardi,[†,‡] Laura Pandolfi,[†,§] Francesca Taraballi,[†] Enrica De Rosa,[†] Iman K. Yazdi,[†] Xeuwu Liu,[†] Mauro Ferrari,[†] and Ennio Tasciotti*[,†]

[†]Department of Nanomedicine, Houston Methodist Research Institute, 6670 Bertner Avenue, Houston, Texas 77030, United States

[‡]Institute of Science and Technology for Ceramics, National Research Council of Italy, Via Granarolo 64, 48018 Faenza, Ravenna, Italy

[§]College of Materials Science and Engineering, University of Chinese Academy of Science, 19A Yuquanlu, Beijing 100049, China

Supporting Information

ABSTRACT: In regenerative medicine, the temporospatially controlled delivery of growth factors (GFs) is crucial to trigger the desired healing mechanisms in the target tissues. The uncontrolled release of GFs has been demonstrated to cause severe side effects in the surrounding tissues. The aim of this study was to optimize a translational approach for the fine temporal and spatial control over the release of proteins, *in vivo*. Hence, we proposed a newly developed multiscale composite microsphere based on a core consisting of the nanostructured silicon multistage vector (MSV) and a poly(DL-lactide-*co*-glycolide) acid (PLGA) outer shell. Both of the two components of the resulting composite microspheres (PLGA-MSV) can be independently tailored to achieve multiple release kinetics contributing to the control of the release profile of a reporter protein *in vitro*. The influence of MSV shape (hemispherical or discoidal) and size (1, 3, or 7 μm) on PLGA-MSV's morphology and size distribution was investigated. Second, the copolymer ratio of the PLGA used to fabricate the outer shell of PLGA-MSV was varied. The composites were fully characterized by optical microscopy, scanning electron microscopy, ζ potential, Fourier transform infrared spectroscopy, and thermogravimetric analysis−differential scanning calorimetry, and their release kinetics over 30 days. PLGA-MSV's biocompatibility was assessed *in vitro* with J774 macrophages. Finally, the formulation of PLGA-MSV was selected, which concurrently provided the most consistent microsphere size and allowed for a zero-order release kinetic. The selected PLGA-MSVs were injected in a subcutaneous model in mice, and the *in vivo* release of the reporter protein was followed over 2 weeks by intravital microscopy, to assess if the zero-order release was preserved. PLGA-MSV was able to retain the payload over 2 weeks, avoiding the initial burst release typical of most drug delivery systems. Finally, histological evaluation assessed the biocompatibility of the platform *in vivo*.

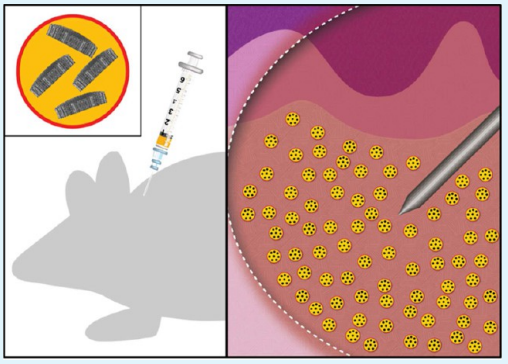

KEYWORDS: *PLGA, silicon, microsphere, drug delivery, tissue engineering*

1. INTRODUCTION

Nanomedicine represents a powerful tool to treat a variety of diseases and recently has become a primary strategy in different applications of tissue engineering.[1] It has become clear that bioactive molecules, such as growth factors (GFs) and cytokines, play a crucial role in orchestrating tissue regeneration.[2] Such a process is led by the immune (e.g., macrophages)[3] and progenitor cells (e.g., mesenchymal stem cells),[4] both of which have been exploited as therapeutic targets.[5] To deliver the bioactive molecules with the correct kinetics it is necessary to trigger the different stages of the regeneration in a temporally controlled fashion.[6] This ensures the right consecution of cellular events necessary to start the healing process (e.g., cell migration, proliferation, and differentiation).[7] The ideal delivery system for tissue engineering should be fully tunable, to allow for the design of virtually infinite possible release kinetics. Furthermore, it should allow for the encapsulation of a high amount of GFs, while preserving their functionality during fabrication. Also, it should ensure the confinement of the bioactive molecules in the site of injection. Although a plethora of carriers for the release of bioactive molecules have been proposed over the past decade, these platforms displayed neither the ideal zero-order release kinetic,[8,9] nor the ability to confine the payload in the target defect for the necessary period of time to allow regeneration.[10] The initial burst release represents a limiting factor in the clinical use of carriers for the release of therapeutic molecules.[11] In fact, it does not allow for control over the daily dose of molecules to be released, and has been shown to cause major side effects.[11] Thus, the ideal carrier

Received: April 21, 2015
Accepted: June 25, 2015
Published: June 25, 2015

DOI: 10.1021/acsami.5b03464
ACS Appl. Mater. Interfaces 2015, 7, 16364−16373

should concurrently confine and retain the biomolecules over time, to preserve the physiology of the surrounding tissues.

Poly(lactic-*co*-glycolic acid) (PLGA) has proven to be a material of choice for the fabrication of delivery systems, such as microspheres, due to its versatile properties.[12−14] It is approved by the Food and Drug Administration and European Medicines Agency for applications of drug delivery due to its biodegradability and biocompatibility and because it also preserves the GFs from degradation.[15−18] Nanostructured porous silicon particles have been widely used in the drug delivery field,[19] for a multitude of applications, ranging from cancer therapy[20] to tissue engineering, where they also proved to be osteoconductive.[21] The main peculiarities of porous silicon particles are that size, shape, porosity, and pore size can be finely tailored during manufacturing.[22] The ability to customize the structure of the particles allows for the control of their biodistribution, bioaccumulation, degradation time, and also the release kinetics. A further degree of control can be applied to the particles' surface: it can in fact be functionalized to include various drugs and control cellular uptake.[23] The highly porous and interconnected structure of the porous silicon particles is suitable to load not only small molecules but also proteins and larger payloads. Porous silicon particles have been efficiently incorporated in a wide range of synthetic polymers in the attempt to introduce a further level of control on the release of the payload.[24,25]

Recently, our group proposed a composite carrier consisting of the nanostructured silicon multistage vector (MSV)[19] and a PLGA outer shell (PLGA-MSV), which, being of great interest in the field of tissue engineering, was demonstrated to allow for the release of high amounts of proteins, while ensuring their stability.[26,27]

The aim of this study was to optimize a translational approach for fine temporal and spatial control over the release of proteins, *in vivo*. Hence, we proposed newly developed multiscale composite microspheres based on a core consisting of the nanostructured silicon MSV and a PLGA outer shell. We investigated the influence of various formulations and fabrication parameters, to allow for the easy translation of this platform to applications of temporospatially controlled release of proteins, for tissue engineering.

2. MATERIALS AND METHODS

2.1. Silicon Particles Fabrication and Surface Modification. Discoidal MSV particles of 1, 3, and 7 μm in diameter and 400 nm thickness or hemispherical particles of 3 μm in diameter and 600 nm thickness were fabricated by photolithography and electrochemical porosification of patterned silicon wafers, allowing for precise control over particle size and shape, as previously reported.[22,27] MSVs were oxidized as extensively described elsewhere.[27,28] Briefly, MSVs were treated with a piranha solution (1 volume of H_2O_2 and 2 volumes of H_2SO_4) with heating to 110−120 °C for 2 h with intermittent sonication to disperse particles. The suspension was then washed in deionized (DI) water until the pH of the suspension was ∼5.5−6. The surface of the MSV particles was modified with (3-aminopropyl)-triethoxysilane (APTES) (Sigma-Aldrich) as previously described.[22] MSV morphology was evaluated by scanning electron microscopy (SEM). Particles were dispersed in DI water, and a drop was deposited on metal stubs. Samples were coated with 3 nm of Pt/Pb and imaged at a voltage of 7 kV (FEI Quanta 400 ESEM FEG, FEI, Hillsboro, OR, USA). Subsequently, 2×10^8 oxidized particles were suspended and mixed in 1 mL of 4% APTES in isopropyl alcohol (IPA) solution and 10% DI in IPA. Particles were mixed at 1300 rpm for 2 h with a thermomixer set at 37 °C and then moved to a vacuum oven for annealing at 60 °C overnight. MSVs were labeled with 4′,6-diamidino-2-phenylindole (DAPI).

2.2. Preparation of PLGA-MSV. MSVs were encapsulated in PLGA particles via a modified double-emulsion method.[29] Several sets of PLGA-MSV composites were created, varying MSV content (2.5, 5, and 10 wt % with respect to the mass of the polymer), MSV shape (hemispherical or discoidal), and MSV size (1, 3, or 7 μm), to evaluate their influence on PLGA-MSV size distribution.

Also, to assess the influence on microspheres' size of the copolymer of PLGA used for the outer shell, three different copolymers were used: 50:50, 75:25, or 85:15. The inherent viscosity of the three copolymers used in this study was 0.55−0.75. In all of the formulations of PLGA-MSV, the PLGA was dissolved in dichloromethane (DCM) at a concentration of 100 mg/mL. Finally, 2×10^8 APTES-modified MSV particles were suspended in 1 mL of the different solutions of PLGA (LACTEL) previously dissolved in DCM, (Sigma-Aldrich). The PLGA outer shell was fluorescently labeled by adding rhodamine B (Sigma-Aldrich) into the PLGA in DCM solution, at a concentration of 1 mg/mL. The organic phase was then emulsified with 3 mL of 2.5% poly(vinyl alcohol) (PVA; Fisher Scientific; 25 mg/mL) at 3000 rpm for 6 min. The emulsion was dropped into 40 mL of a 1% aqueous solution of PVA (10 mg/mL). The resulting phase was stirred overnight to allow DCM evaporation; particles were then washed three times with DI water and collected via centrifugation for lyophilization and long-term storage.

2.3. Characterization of PLGA-MSV. Full encapsulation of MSV microparticles in the PLGA microspheres was assessed by optical microscopy. The effect of MSV content, shape, and size and PLGA copolymer ratio on PLGA-MSV size was investigated by measuring the diameter of the microspheres by an automated measuring tool of the software NIS element (Nikon). The ζ potential of the silicon particles, prior to encapsulation in the PLGA shell, was analyzed using a Zetasizer nano ZS (Malvern Instruments Ltd., Southborough, MA, USA), as previously described.[26] APTES-modified MSV and the resulting PLGA-MSV microspheres were analyzed by Fourier transformed infrared spectroscopy (FTIR). Briefly, a KBr pellet was made by mixing KBr to freeze-dried PLGA-MSV. The KBr chip was analyzed by a Nicolet 6700 spectrometer (Thermo Scientific). The MSV content in the composite microspheres was characterized by thermogravimetric analysis (TGA), while the thermal properties of PLGA-MSV were evaluated by differential scanning calorimetry (DSC) through the Q600 TG-DSC apparatus (TA Instruments).

2.4. Loading of FITC-BSA into APTES-Modified MSV Particles and Encapsulation in PLGA Shell. In order to load the selected reporter protein, APTES-modified MSV particles were suspended in 500 μL of solution of FITC-BSA (Sigma-Aldrich) in DI (10 mg/mL). The suspension was incubated in physiological-like conditions (PBS, 37 °C, under mild agitation). Centrifugation at 4000 rpm for 5 min allowed for the isolation of the particles. The collected supernatant has been used to estimate the amount of protein absorbed by mass difference using a spectrophotometer SpectraMax M2 (Molecular Devices) at 493 nm/518 nm. The FITC-BSA-loaded particles were then lyophilized overnight. FITC-BSA-loaded MSV were encapsulated in a PLGA shell, as described above. BSA loading was also evaluated by imaging PLGA-MSV by an A1 confocal laser microscopy (Nikon).

2.5. Evaluation of FITC-BSA *in Vitro* Release. After dispersing in PBS (1.5 mL), 2×10^8 FITC-BSA-loaded PLGA-MSV microspheres were divided into three aliquots: each sample contained approximately 7×10^7 particles suspended in 0.5 mL of PBS. Samples were collected, at established time intervals, for 1 month. Each sample was centrifuged (4000 rpm; 5 min), and 10% of the supernatant (0.05 mL) was collected and replaced with fresh PBS. The release of FITC-BSA from the different formulations of PLGA-MSV was quantified by a spectrophotometer at 493 nm/518 nm. Samples were collected and analyzed at defined time points, up to 1 month.

2.6. Biocompatibility Study. J774 macrophages were utilized for this study (ATCC). Briefly, murine J774 macrophages (J774) were cultured according to vendor's protocols (ATCC), in HG-DMEM supplemented with 10% FBS, 1% penicillin (100 UI/mL)-streptomycin (100 mg/mL), and 0.25 mg/mL amphotericin B. J774 cells were

DOI: 10.1021/acsami.5b03464
ACS Appl. Mater. Interfaces 2015, 7, 16364−16373

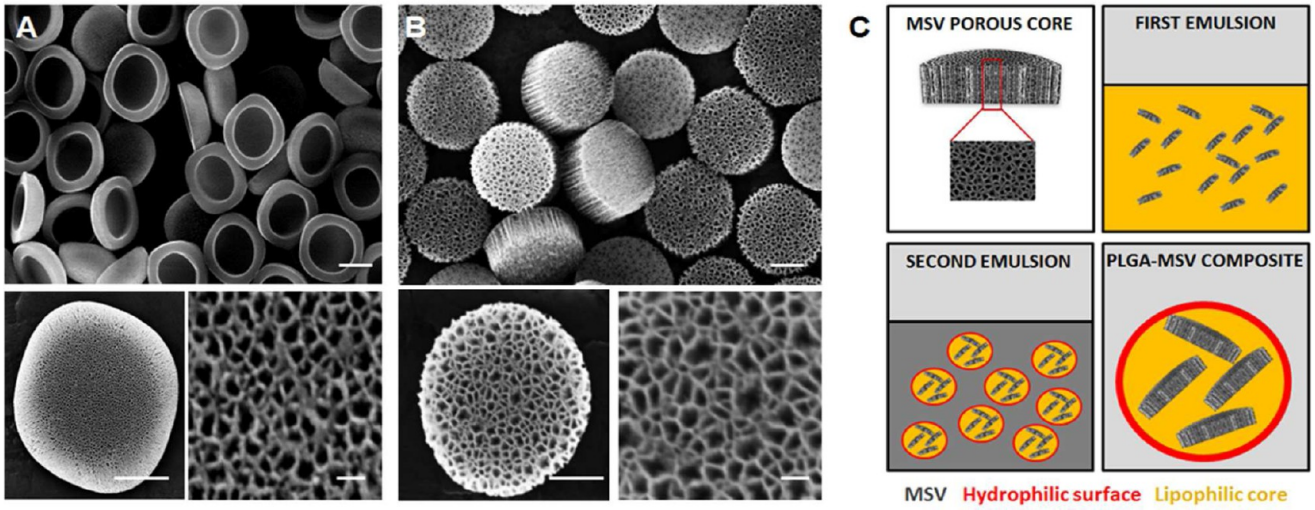

Figure 1. SEM images of hemispherical and discoidal MSV particles, including the close-up view of a single particle and of its pores (A, B respectively). The overall sizes of the particles are the same, but the shape is significantly different. Scale bar, 1 μm; scale bar of the close up of the pores, 100 nm. Schematic showing the steps of PLGA-MSV fabrication with the double-emulsion technique (C).

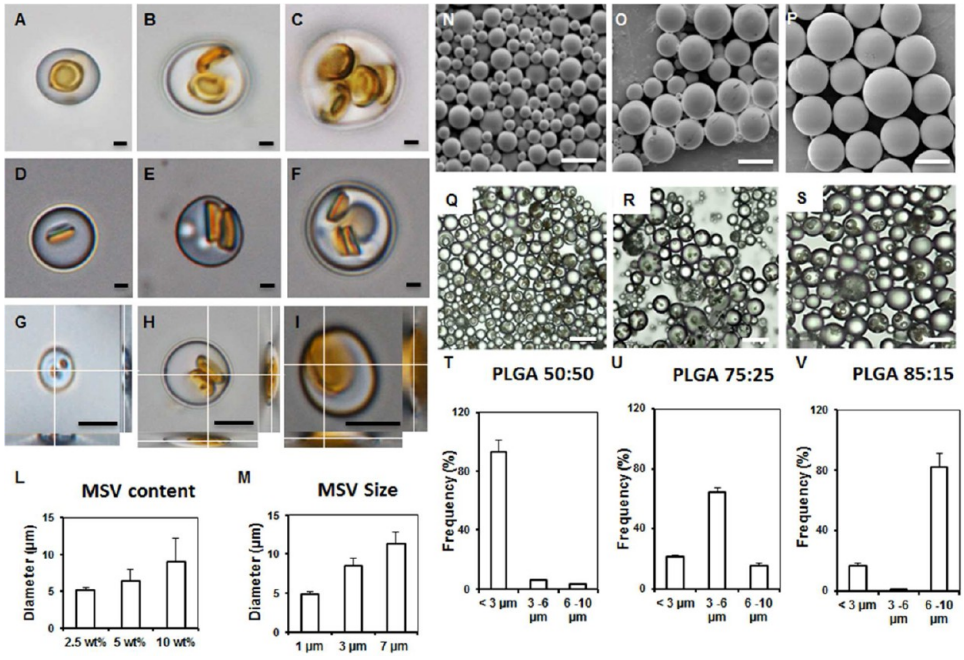

Figure 2. Optical microscopy images of PLGA-MSV with increasing amount of hemispherical MSV (A, B, C) or discoidal MSV (D, E, F). Images of PLGA-MSV fabricated with discoidal MSV of increasing diameter (G, H, I): scale bars, 1 μm. Quantification of PLGA-MSV diameter depending on MSV content (L) or MSV size (M). SEM and optical microscopy images (N, O, P and Q, R, S respectively) of PLGA-MSV fabricated with 50:50, 75:25, or 85:15 PLGA coatings: scale bars ,10 μm. Bar graphs reporting the size distribution of PLGA-MSV prepared with different copolymer ratios of PLGA (T, U, V).

subcultured by plating them into 96-well plates at a density of 5000 cells/cm^2 (Millipore). After 24 h, cells were treated with PLGA-MSV with PLGA at 50:50, 75:25, and 85:15 and fabricated with all sizes of MSV (1, 3, and 7 μm). Five different concentrations of microspheres were tested, ranging between 0.1 and 10 μg/mL. Viability was evaluated at 72 h, in triplicate. Cell interaction with PLGA-MSV was initially evaluated by SEM, and samples were prepared for imaging as previously described (FEI Quanta 400 ESEM FEG, FEI).[30] Samples were vacuum-dried and coated with Pt/Pb and imaged by SEM under a voltage of 8 kV (Hummer 6.2 sputtering system; Anatech Ltd., Union City, CA, USA). The toxicity of the different formulations and concentrations of PLGA-MSV described previously was evaluated by MTT assay, according to manufacturer's protocol (Life Technology).

2.7. Subcutaneous Injection. Twenty-eight BALB/c mice (8−12 weeks old) were housed and fed in the animal room at The Houston Methodist Research Institute (Houston, TX, USA) for 48 h prior to the experiment. The study protocols were approved by the Institutional Animal Care and Use Committee (IACUC) and performed following GMP standards. All efforts were made to minimize the number of animals used for experiments and their suffering. Animals were anaesthetized with 2−3% isoflurane in 100% oxygen at a flow rate of 1 L/min. A 1 cm^2 area of skin was carefully shaved and sterilized. Mice were injected at a dorsal subcutaneous site with 50 μL of a PLGA-MSV suspension in PBS. Seven animals per each time point were used. In each animal two injections were performed: one as a control (PBS only) and one with the PLGA-MSV suspension. Mice were euthanized at 2 h

DOI: 10.1021/acsami.5b03464
ACS Appl. Mater. Interfaces 2015, 7, 16364−16373

and 3, 7, and 14 days, by CO_2 inhalation and subsequent cervical dislocation.

2.8. *In Vivo* Release Study. One mouse per each time point was imaged by intravital microscopy (IV), prior to being euthanized, to follow the *in vivo* release of the reporter protein. Briefly, the skin was gently dissected, flipped, and imaged at three wavelengths: 610 nm for PLGA microsphere (labeled with rhodamine B), 460 nm for MSV particles (labeled with DAPI), and 516 nm for FITC-BSA. Regions of interest were created with a specific tool of the software NIS-Element (Nikon) to evaluate the diffusion of BSA from the microspheres and to verify the confinement of the carriers over 2 weeks.

2.9. *In Vivo* Degradation of PLGA-MSV. The tissue surrounding the injection site was collected (0.5 cm × 0.5 cm) and fixed for SEM images in 2.5% glutaraldehyde and prepared for SEM evaluation. The tissues were dehydrated in increasing concentration of ethanol (EtOH), as described elsewhere.[29] Samples were sputter-coated with 25 nm of Pt/Pb and imaged with a voltage of 10 kV, to evaluate the *in vivo* degradation of the carriers.

2.10. Biodistribution. The mice organs and the tissues surrounding the injection site (0.5 cm × 0.5 cm) were collected and homogenized in 20% EtOH in 1 M NaOH and incubated under mild agitation for 24 h at room temperature, to further verify confinement of the microspheres. Weighed organs (lungs, liver, kidneys, and spleen) and the tissue surrounding the site of injection were then centrifuged at 5000 rpm for 30 min and supernatant was collected, filtered using 0.45 μm nylon centrifugal filter microfuge tubes (VWR), and diluted with DI for elemental analysis by ICP-OES (Varian 720 ES, Varian Inc., Walnut Creek, CA, USA) as previously described.[23]

2.11. Histological Evaluation. At each time point, the tissue surrounding the site of injection (PLGA-MSV), or PBS for the control sample, was collected and fixed in OCT mounting media (Tissue Tek, SAKURA) for histology. Briefly, samples were cut 10 μm thick, and sections were washed twice in fresh xylene for 8−10 min and rehydrated sequentially with decreasing ethanol concentrations (100%, 95%, 90%, 80%, and 70%) and DI water (8−10 min for each step). Histological visualization of collagenous connective tissue fibers in tissue sections was achieved using a commercially available kit for Trichrome stain (Abcam; ab150686), according to the manufacturer's instructions. The air-dried slides were then mounted with Cytoseal XYL (Thermo Scientific) mounting medium and then analyzed by Nikon histological microscope.

2.12. Statistical Analysis. Statistics were calculated with Prism GraphPad software. Statistics for experiments were performed using a two-way ANOVA followed by a Tukey's multiple comparison test. In all cases * was used for $p < 0.05$, ** for $p < 0.01$, and *** for $p < 0.001$, and **** for $p < 0.0001$. All experiments were performed at least in triplicate. Data are presented as mean ± SD.

3. RESULTS AND DISCUSSION

3.1. Morphological and Chemical Characterization of PLGA-MSV. The ability to finely control the shape and size of a carrier for bioactive molecules is crucial to ensure a tight control over the physicochemical properties of the system, its loading efficiency, and ultimately its ability to control spatially and temporally the release of its payload. In this study, we investigated the tunability of a composite carrier based on a MSV core and an outer PLGA shell. Both components are fully tunable and can be tailored to address any clinical need. The main aim of this study was to elucidate the role of several fundamental variables during PLGA-MSV synthesis (e.g., shape, size, and amount of MSV, and PLGA copolymer ratio), to make it a user-friendly platform and clinically translational.

First, we investigated the influence of MSV shape on PLGA-MSV's morphology and size distribution. Thus, we fabricated hemispherical and discoidal MSV (Figure 1A,B), with a diameter of 3 μm. MSVs were synthesized through an optimized lithographic method,[22] resulting in particles with a porosity of 51%. This process is scalable and reproducible, giving MSVs of uniform shape and size, which is crucial in ensuring control over the loading and release of the payload. A modified double-emulsion method was followed to fully encapsulate the MSV in the PLGA microspheres (Figure 1C), creating composite microspheres. PLGA was chosen to synthesize the outer shell of the composite microspheres, as it is commercially available in a wide range of copolymer ratios, molecular weights, and viscosities, which influence the degradation rate of the polymer *in vitro* and *in vivo*, by modulating its hydrophilic properties.[31,32]

Table 1. ζ Potential Values Measured by DLS, of Oxidized MSV (Negatively Charged) and APTES-Modified MSV (Positively Charged)

run	ζ potential	rel residual
	Oxidized MSV	
1	−30.313	0.019
2	−30.113	0.014
3	−30.772	0.022
mean	−30.393	0.018
SD	0.343	0.004
	APTES-Modified MSV	
1	6.825	0.006
2	6.82	0.008
3	6.593	0.009
mean	6.737	0.008
SD	0.127	0.001

By varying the content of MSV (hemispherical, Figure 2A−C; discoidal, Figure 2D−F) during the synthesis (2.5, 5, and 10 wt %), we observed similar morphology and an increase in the diameter of the resulting PLGA-MSV composite microspheres: 5.103 ± 0.373) μm for the 2.5 wt % MSV in PLGA, 6.435 ± 1.494 μm for the 5 wt % MSV in PLGA, and 9.013 ± 3.230 μm for the 10% MSV in PLGA. Similarly, by utilizing discoidal MSV of increasing diameter (1, 3, and 7 μm) the mean size of the resulting microspheres increased accordingly, as well (Figure 2G−I). The mean diameter of all of the previously mentioned formulations of PLGA-MSV are reported in the bar graphs in Figure 2L,M. The formulation that produced PLGA-MSV with the lowest standard deviation was the 2.5 wt % 1 μm discoidal PLGA-MSV; thus as a proof of concept we continued our study with 1 μm discoidal MSV. However, we emphasize how all formulations were characterized by relatively low standard deviations, showing the ability to produce homogeneous batches of PLGA-MSV.

After investigating the effect of different shapes, amounts, and sizes of MSV, on the overall morphology and size distribution of the resulting PLGA-MSV, we wanted to study the influence of the formulation of the PLGA shell on the resulting composite microspheres.

We tested three copolymer ratios of PLGA: 50:50, 75:25, and 85:15. At higher copolymer ratios the overall size of PLGA-MSV increased (Figure 2N−P) and resulted in the microspheres shown in Figure 2Q−S. PLGA-MSV fabricated with 50:50 and 85:15 copolymers displayed a superior size distribution with respect to those made with 75:25 PLGA, which appeared to include three distinct subpopulations of microspheres; thus, we selected 85:15/1 μm discoidal PLGA-MSV for further characterization, as a proof of concept. Overall, this first part of our study, demonstrated how our PLGA-MSV composite delivery system is

DOI: 10.1021/acsami.5b03464
ACS Appl. Mater. Interfaces 2015, 7, 16364−16373

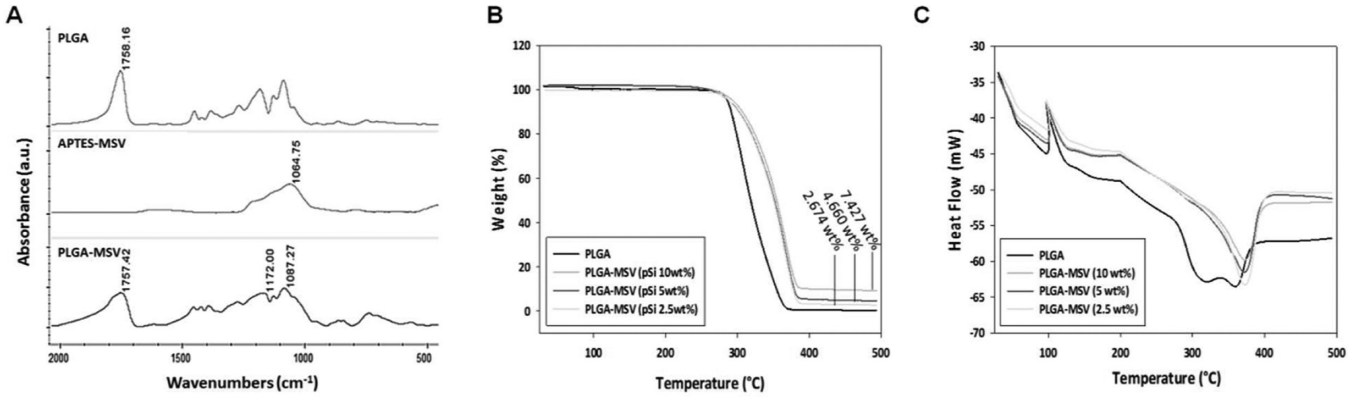

Figure 3. FTIR spectra of PLGA microspheres, APTES-modified MSV, and PLGA-MSV composite microspheres. The peaks corresponding to the major chemical species identified in the samples were labeled. (A) Thermogravimetric analysis determining the weight loss of organic fraction from the tested samples, to characterize the amount of MSV in the three formulations of composite microspheres (B). Differential scanning calorimetry showing the melting process of the three formulation of PLGA-MSV, made with a decreasing amount of MSV, compared to empty PLGA microspheres (C). While the PLGA microspheres displayed the typical degradation process, the composite microspheres had a very different melting process, as more energy was needed to degrade the PLGA-MSV with higher amounts of MSV.

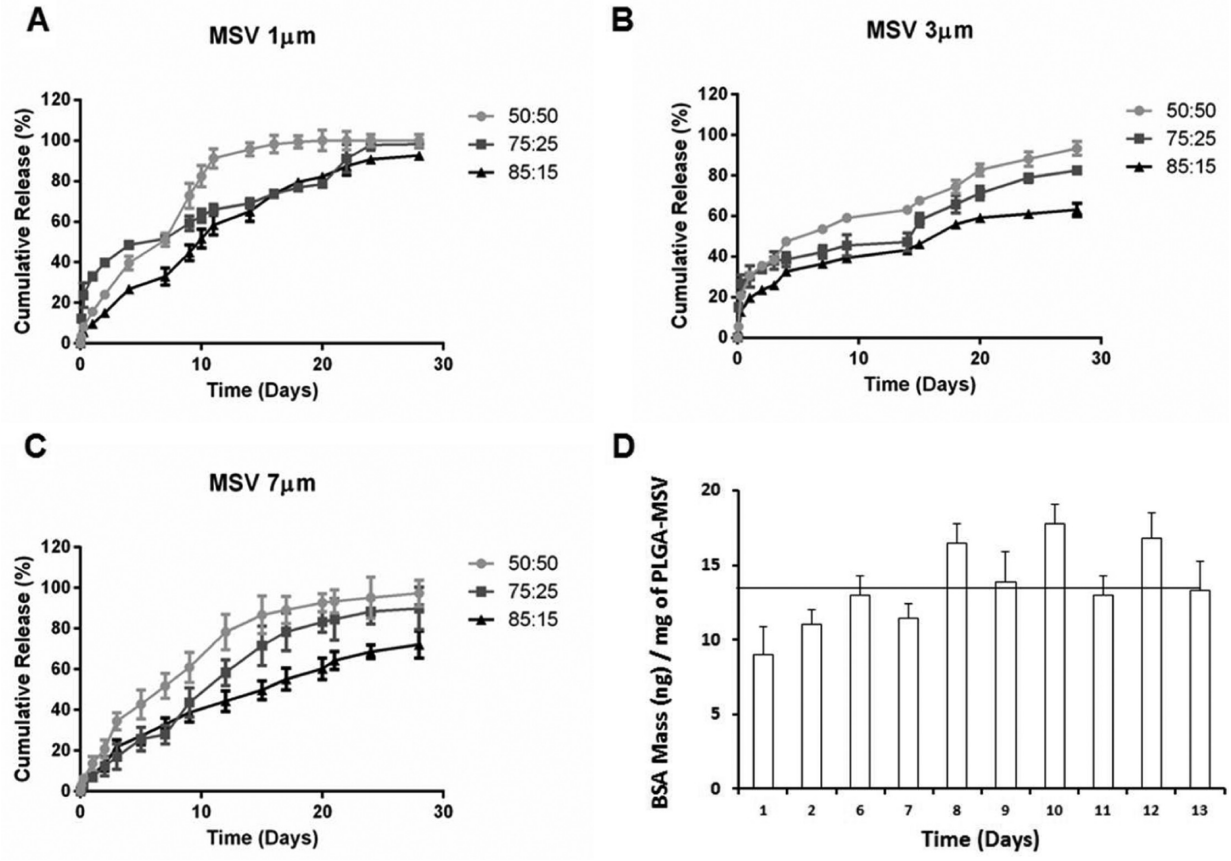

Figure 4. Time-dependent release of FITC-BSA from PLGA-MSV. Nine different formulations of PLGA-MSV were prepared and were loaded with the reporter protein, and the mean fluorescence of their supernatants was measured over time: 50:50, 75:25, and 85:15/(1 μm PLGA-MSV) (A); 50:50, 75:25, 85:15/(3 μm PLGA-MSV) (B); 50:50, 75:25, 85:15/(7 μm PLGA-MSV) (C). The release was expressed as a percentage of the total amount of the payload released from the microspheres. Bar graph reporting the daily mass of BSA released from the 85:15 per 1 μm PLGA-MSV (D). This PLGA-MSV formulation allowed for the release of an interestingly consistent daily dose of protein, as desired.

advantageous in that it can be fully customized to match the user's needs.

In order to diminish the hydrophobicity of the particles and enhance their loading efficiency, the particles' surface was first oxidized by etching.[19] This step allowed for the introduction of hydroxyl groups on the surface of the silicon particles, which were further functionalized with primary amine groups by surface modification with APTES. ζ potential analysis showed a mean surface charge of 6.737 mV after APTES modification, versus the initial value of −30.39 mV (Table 1). The surface charge affects the loading efficiency of bioactive proteins.[26] BSA, in fact, had a negative charge and the electrostatic interaction

DOI: 10.1021/acsami.5b03464
ACS Appl. Mater. Interfaces 2015, 7, 16364−16373

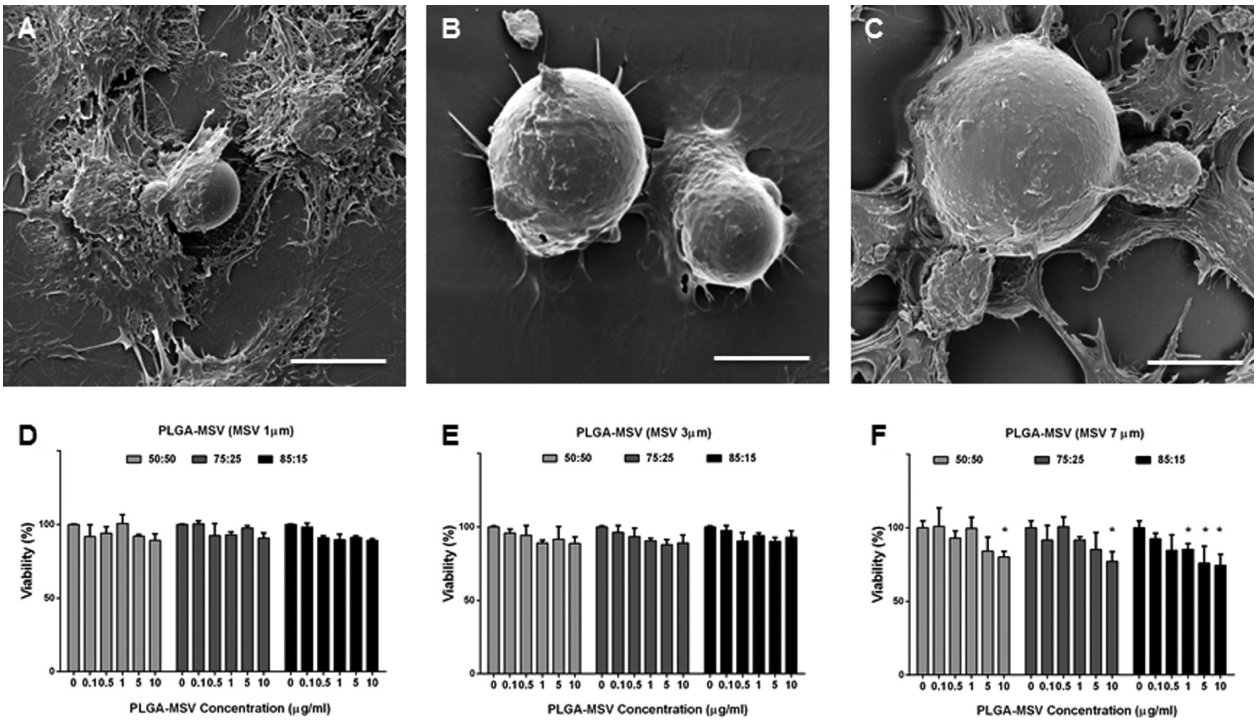

Figure 5. SEM images of J774 interacting with PLGA-MSV fabricated with MSV 1 (A), 3 (B), and 7 μm (C). Depending on the size of PLGA-MSV the cells behaved differently; in particular J774 were easily able to interact and internalize PLGA-MSV fabricated with 1 and 3 μm MSV. However, it appeared that J774 were not able to engulf PLGA-MSV fabricated with MSV 7 μm, but rather surrounded them. Viability study by MTT assay of J774 incubated with increasing concentrations of 50:50, 75:25, 85:15 PLGA-MSV with 1 μm, 3 μm, and 7 μm MSV (D, E, F): scale bars, 5 μm. No significant differences in the viability of cells were found among the tested groups of PLGA-MSV, with MSV 1 and 3 μm. On the contrary, the viability of J774 was slightly decreased when cells were incubated with PLGA-MSV 7 μm.

between amine groups of APTES and acidic moieties of BSA intensified the ability of FITC-BSA to be loaded into the pores of MSV particles, allowing for an average loading efficiency over 80.33 ± 3.19% (Supporting Information Figure S1).

Second, we verified the formation of a real composite between the inorganic (MSV) and organic (PLGA) phase: FTIR spectra revealed a stretching of the carboxylic groups of amide I of PLGA-MSV (1735−1750 cm^{-1}), and a broadening of the peaks in the ranges 1580−1650 cm^{-1} (N−H bend of primary amines) and 665−910 cm^{-1} corresponding to N−H wag of primary and secondary amines, suggesting an ionic interaction of the carbonyl groups on the surface of the PLGA with the amine groups of APTES-modified MSV (Figure 3A). The most important advantage of composite delivery systems is related to their unique degradation mechanism, as it is slower and more sustained. The byproducts produced by the degradation of MSV and PLGA act as a buffer, producing a neutral pH, avoiding protein degradation.[27] Thus, by blending MSV and PLGA (inorganic/organic composite), it is possible to obtain a composite that is more stable when exposed to the fluctuation of the microenvironment of tissues, better protecting the payload.[29] TGA analysis was performed for 85:15/1 μm discoidal PLGA-MSV with different amounts of MSV (2.5, 5, and 10 wt %) and resulted in 2.674, 4.660, and 7.427 wt %, respectively (Figure 3B). From DSC analysis an increase in the T_m of PLGA-MSV was observed with respect to that of empty PLGA microspheres (used as a control) of approximately 15 °C, proving the existence of a chemical interaction between MSV and the polymer, thus further proving the formation of an actual composite. Also among the three formulations of PLGA-MSV, the heat flow value of those endothermic reactions that resulted progressively decreased at higher contents of MSV (Figure 3C).

3.2. Evaluation of FITC-BSA Release Kinetics *in Vitro*.

The release of FITC-BSA was assessed over a month (Figure 4). Evidence resulting from the release study demonstrated that the increase of the copolymer ratio of the PLGA coating enabled the progressive reduction of the initial burst release (higher R^2) and a slower release rate (lower angular coefficient of the trendline interpolating the release curves). This was further supported by the fact that FITC-BSA was found to be secured in correspondence with the MSV core, and thus protected from the environment, avoiding massive burst release (Supporting Information Figure S2).

Also, we found that the bigger the size of the MSV microspheres utilized in the preparation of the PLGA-MSV, the slower the release of the reporter protein. It is possible to observe that both 85:15/1 μm PLGA-MSV and 85:15/7 μm PLGA-MSV allowed for almost zero-order release kinetics. However, with the bigger size of MSV (7 μm), there was a higher variability in the amount of protein released daily (Figure 4A,C). Thus, the 85:15/1 μm PLGA-MSV formulation allowed for the most sustained, controlled, and consistent release (lowest standard deviations, lower slope, and higher R^2; see Supporting Information Figure S3), with an almost zero-order kinetic, releasing approximately 12.845 ± 0.987 ng/day (Figure 4D).

The release kinetics of BSA from PLGA-MSV synthesized with 1 μm MSV were the most affected by the copolymer ratio utilized in the preparation of the composite microspheres. The PLGA-MSV prepared with the 50:50 copolymer had the fastest release rate and an evident burst release. Similarly, PLGA-MSV made with the 75:15 PLGA copolymer had a notable initial burst

DOI: 10.1021/acsami.5b03464
ACS Appl. Mater. Interfaces 2015, 7, 16364−16373

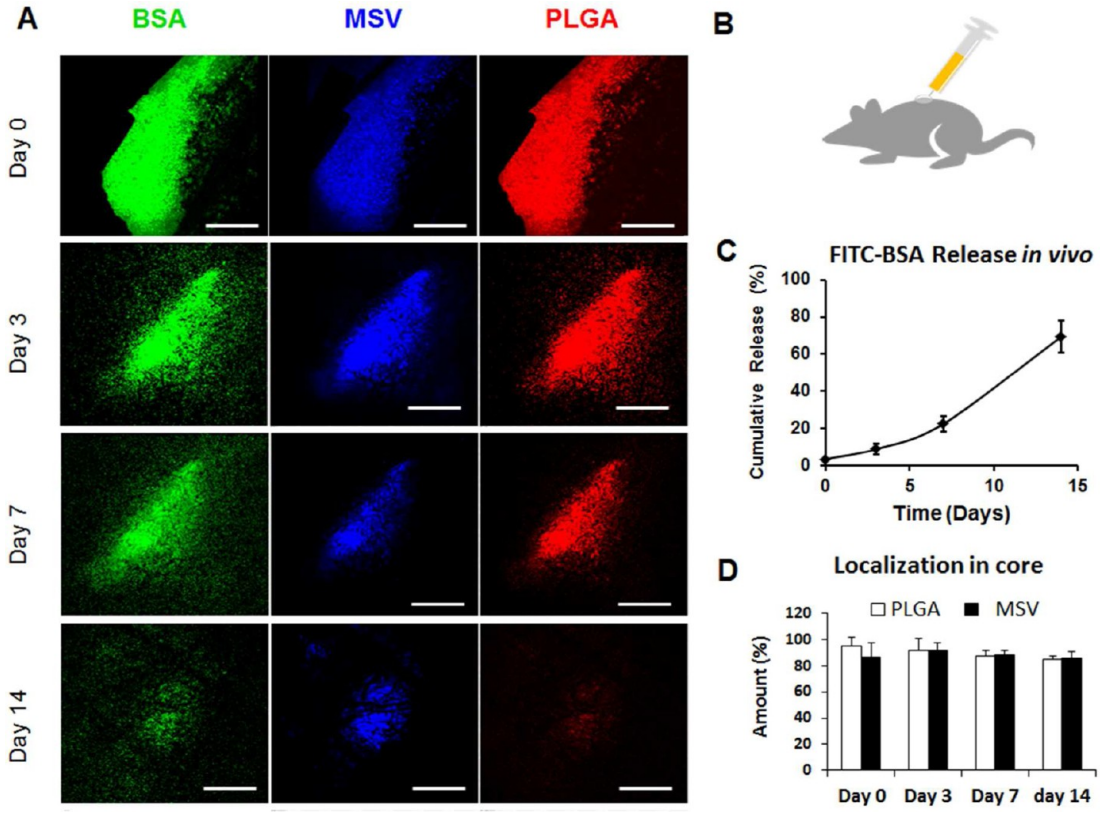

Figure 6. Intravital microscopy images of FITC-BSA-loaded PLGA-MSV, showing the *in vivo* release of BSA, in a subcutaneous model in mice (FITC-BSA, green; MSV, blue; PLGA microspheres, red) (A). Site of the injection of PLGA-MSV, in the back of the mouse (B). As expected, BSA is progressively released in the surrounding of the PLGA-MSV signal. MSV and PLGA fluorescent signals appeared to remain colocalized over time. Release kinetic of FITC-BSA *in vivo*, over 2 weeks, confirming the zero-order release kinetics (C). Amount of MSV particles and PLGA microspheres localized in the site of injection, over time, showing that PLGA-MSV remains localized in the desired site (D).

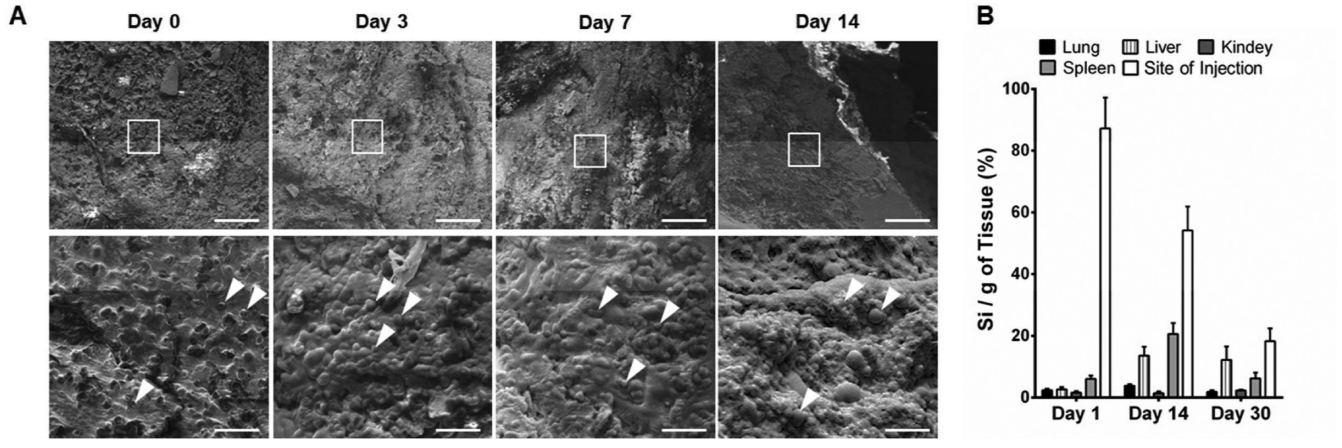

Figure 7. SEM micrographs at 0, 3, 7, and 14 days after injection, of the PLGA-MSV in the mice subcutaneous model, showing *in vivo* degradation of the microspheres (A): top images scale bars, 100 μm; insets scale bars, 20 μm. The white arrows in the insets indicate single PLGA-MSV. Biodistribution of MSV in lung, liver, kidney, spleen, and tissue surrounding the injection site, in mice, up to 30 days (B), showing that most of the PLGA-MSV remains in the site of injection.

release, but the release rate slowed down after day 7. No significant differences were found among the different formulations of PLGA-MSV prepared with 3 μm MSV, in terms of kinetics; however, we can observe that the higher the copolymer ratio, the slower the release. Similarly, at higher copolymer ratios the release was slower for PLGA-MSV 7 μm.

The temporal control over the release of the payload is fundamental to guarantee the proper therapeutic effect, for the necessary window of time. In fact, the tight regulation of the dose of bioactive molecule released daily allows for the avoidance of side effects due to overdoses or the progression of the pathological state due to an insufficient amount of drug. For these reasons, as a proof of concept, we chose the 85:15/1 μm PLGA-MSV formulation to be tested for its release in a mouse subcutaneous model, in the attempt to verify if the zero-order release was preserved in *in vivo* conditions.

DOI: 10.1021/acsami.5b03464
ACS Appl. Mater. Interfaces 2015, 7, 16364−16373

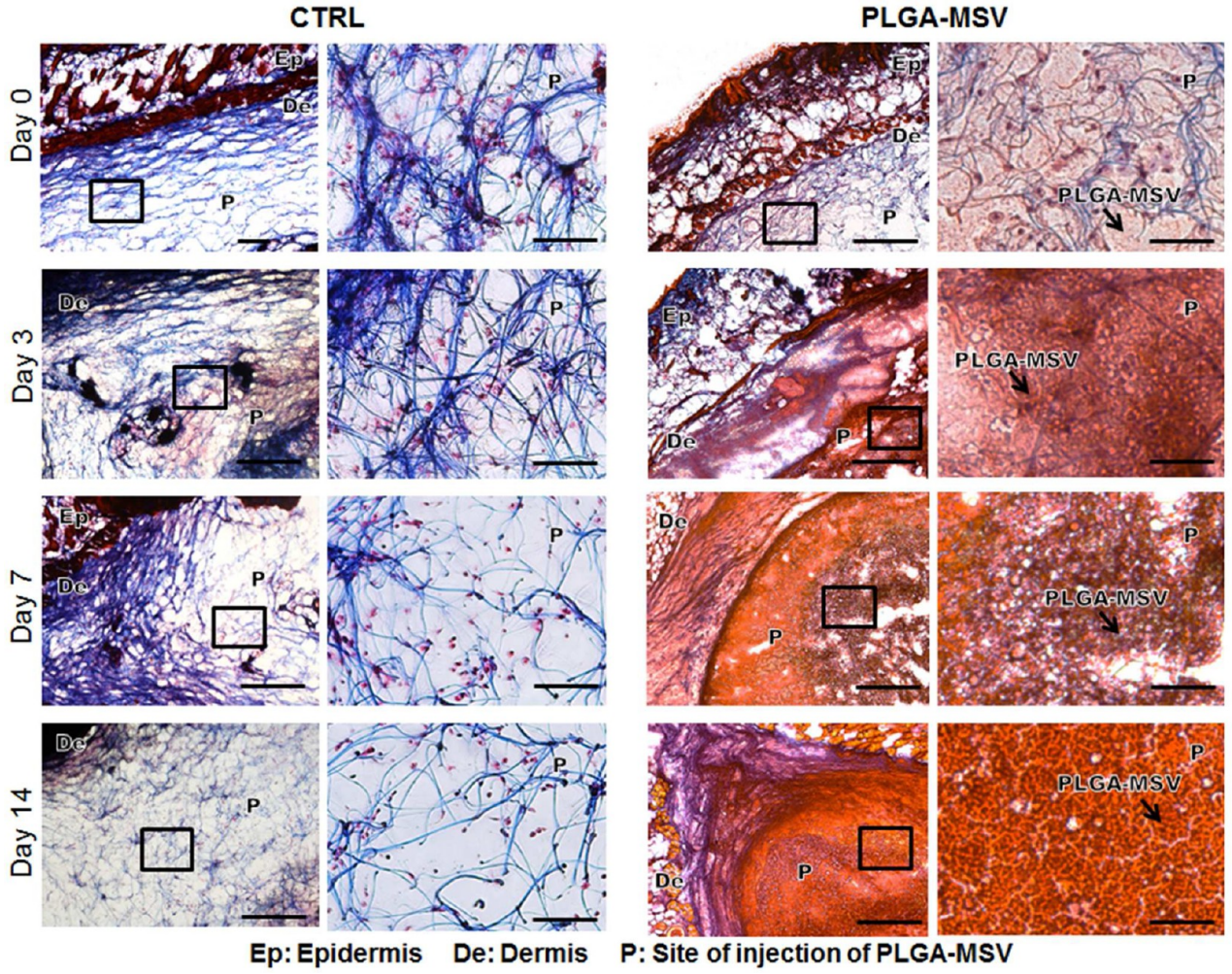

Figure 8. Trichrome histological evaluation at 0, 3, 7, and 14 days of the *in vivo* reaction to the PLGA-MSV, injected subcutaneously in mice. Control mice were injected with PBS and compared to the mice injected with PLGA-MSV. Scale bars of low magnification images, 300 μm; insets, 50 μm. The images of the controls present fibers and a minor accumulation of cells, which resolved over the 2 weeks. In the tissue surrounding the injection site of PLGA-MSV (P), the accumulation of fibers (in blue) and of a few cells was observed, similarly to what was found in the control samples. The PLGA-MSV (red) were identified at each time point, to still be in the site of injection, further confirming the spatially controlled release.

3.3. Biocompatibility. Macrophages have been demonstrated to be one of the first types of immune cells to intervene at the site of injury.[33] Thus, we simulated the *in vitro* response to the PLGA-MSV by incubating murine macrophages with increasing concentrations of PLGA-MSV fabricated with MSV 1, 3, or 7 μm (PLGA-MSV of increasing size) (Figure 5A–C). The viability of macrophages was not significantly compromised by increasing concentrations of PLGA-MSV made with 1 and 3 μm MSV (Figure 5D, E). We observed that with PLGA-MSV made with 7 μm MSV, macrophage viability slightly decreased by increasing the amount of PLGA-MSV in the media, but remained above 80% (Figure 5F). We verified that the biggest PLGA-MSVs were not internalized but rather surrounded by the macrophages (Figure 5C), as extensively reported.[32,34]

3.4. *In Vivo* Spatially Controlled Release. Ultimately, we wanted to assess if the ability to control the spatial and temporal control over the release of FITC-BSA accomplished *in vitro* was preserved *in vivo*. The release of the reporter protein was followed over 14 days, in a mouse subcutaneous model, by intravital microscopy. In Figure 6 the images acquired by intravital microscopy are presented. The panel shows that both PLGA (red) and MSV (blue) signals overlap for all of the windows of time considered. This was further demonstrated by the fluorescence intensity plot, in which the fluorescence signals of the three components of the carrier not only overlap, but show that the outer layer of the system is the PLGA (red), the middle one is MSV (blue), and the inner component is the FITC-BSA (green) (Supporting Information Figure S4). Concerning FITC-BSA, it is possible to identify a slight diffusion of the protein outside the area where PLGA-MSVs were localized. However, the BSA diffused in the immediate surroundings of the microspheres (distributed over an area of 1.148 mm^2) over a maximum area of 4.778 mm^2, thus demonstrating the ability of PLGA-MSV to retain FITC-BSA at the earliest time point, avoiding the initial burst release *in vivo*, as characterized *in vitro*.

After intravital microscopy analysis, the tissue surrounding the injection site was imaged by SEM, to better evaluate the morphology and degradation of PLGA-MSV. Figure 7A depicts the microspheres after injection, at day 3, 7, and 14. At all time points it is possible to identify PLGA-MSV microspheres, as indicated by the white arrows.

If internalized by phagocytes (see section 3.3), PLGA-MSV would be transported to the spleen, or the kidney. We finally

DOI: 10.1021/acsami.5b03464
ACS Appl. Mater. Interfaces 2015, 7, 16364–16373

evaluated the spatial control over the payload by evaluating the confinement of MSV in the tissue surrounding the injection site. ICP analysis of the content of Si in the organs of the mice showed that at day 1 more than 85% of Si was found in the site of injection, while progressively decreasing over a month (54% at 14 days and 18% at 30 days), mirroring the sustained release of the protein *in vitro* (Figure 7B).

However, it has been extensively demonstrated that MSV degradation in biological conditions occurs faster in cancer therapy[35,36] than what is needed for tissue engineering applications, inciting the need for the inclusion of MSV in polymer shells or scaffolds.

Panels in Figure 8 show the histological evaluation of the tissue surrounding the injection site up to 14 days after injection, compared to the control. The images of the controls immediately after injection of saline solution presented fibers and a minor accumulation of cells, which resolved over the 2 weeks evaluated. At day 0, in the tissue surrounding the injection site of PLGA-MSV, the accumulation of fibers (blue) and of a few cells was observed, similarly to what was found in the control samples. Within 2 weeks the outer polymeric shell (TRITC-labeled) started to slowly degrade, and release part of the dye, as evidenced by the more intense red color of the slides. Altogether these data confirm the controlled process of degradation of PLGA-MSV *in vivo*, which is reflected in a slow and sustained release of the reporter protein, within the tissue surrounding the injection site.

Drug delivery systems, alone or combined with tissue engineering devices and scaffolds, are promising approaches for the treatment of a multiplicity of damaged tissues.[37,38] However, their clinical use has been limited by a number of challenges, including the inability to accurately control the spatial and temporal release of GFs *in vivo*. In fact, the initial burst release of drugs from the currently available systems and devices represents the most limiting factor in their clinical use.[11] A notorious controversy spurred over the release of GFs in tissue engineering applications, when Medtronic developed INFUSE, a collagen sponge impregnated with a solution of recombinant human bone morphogenic protein-2 for bone augmentation. Although the market leader for years, this product has been associated with several disruptive patients' complications (e.g., osteolysis, heterotopic ossification, and even cancer).[39,40]

With the recent advances in biology, chemistry, and materials science, polymeric materials can now be synthesized from a combinatorial array of monomers, oligomers, and polymers with tunable chemical, mechanical, and geometrical properties to create new, biocompatible substances.[41,42] In our study we proposed a composite polymer/silicon delivery system that was demonstrated to be fully tunable, with a slow and controlled degradation process which allows for a long-term release, *in vivo*. Also, our platform is highly reproducible, and not toxic, as shown by the biocompatibility study and biodistribution (very little PLGA-MSV was transported to the filtrating organs for excretion). Remarkably, for the first time it was demonstrated that it is possible to obtain a zero-order release of proteins *in vivo*, with our PLGA-MSV.

4. CONCLUSIONS

In summary, we have demonstrated the full tunability of PLGA-MSV composite microspheres. This kind of composite carrier combines the advantages of mesoporous structures which can be loaded with a high amount of proteins, due to their high surface area, and the plasticity and tailorability of polymers. In this study the formulation which accomplished a zero-order release (85:15/1 μm PLGA-MSV) was tested in a mouse subcutaneously, to demonstrate the ability of this platform to accomplish the temporal and spatial control over the release of its payload. It is possible to envision the use of the different formulations of PLGA-MSV for the staged release of multiple factors, to closely mimic the natural temporal gradients of biomolecules. It is greatly advantageous that PLGA-MSV are injectable, which allows for easy administration of the payload, once a month, with low toxicity. These results demonstrated *in vivo* that PLGA-MSV represents a robust, reproducible, and scalable platform to be translated in the clinic, for applications of tissue regeneration.

■ ASSOCIATED CONTENT

Supporting Information

(Figure S1) Mean loading efficiency and mass of protein loaded in the MSV particles of 1, 3, or 7 μm, (Figure S2) confocal laser microscopy images of PLGA-MSV loaded with FITC-BSA, (Figure S3) trendline interpolating the release curves, (Figure S4) fluorescence intensity plot of the tissue surrounding the site of injection of PLGA-MSV for the wavelength of the three components of the system, TRITC (PLGA), DAPI (MSV), and FITC (BSA). The Supporting Information is available free of charge on the ACS Publications website at DOI: 10.1021/acsami.5b03464.

■ AUTHOR INFORMATION

Corresponding Author

*Phone: +17134417319. E-mail: etasciotti@tmhs.org.

Funding

This study was supported by the Brown Foundation (Project ID, 18130011) and by the Cullen Trust for Health Care Foundation (Project ID, 18130014).

Notes

The authors declare no competing financial interest.

■ ACKNOWLEDGMENTS

We thank Dr. J. Gu of the HMRI Microscopy-SEM/AFM core and the HMRI Pathology core for cutting the histological specimens. We thank Matt Landry for assistance with the schematic and Zachary Mills for support with editing of the English.

■ ABBREVIATIONS

MSV, nanostructured silicon particles
PLGA, poly(DL-lactide-*co*-glycolide) acid
PLGA-MSV, PLGA-porous silicon particles composite microspheres

■ REFERENCES

(1) Chaudhury, K.; Kumar, V.; Kandasamy, J.; RoyChoudhury, S. Regenerative Nanomedicine: Current Perspectives and Future Directions. *Int. J. Nanomed.* **2014**, *9*, 4153.

(2) Lee, K.; Silva, E. A.; Mooney, D. J. Growth Factor Delivery-Based Tissue Engineering: General Approaches and a Review of Recent Developments. *J. R. Soc., Interface* **2011**, *8* (55), 153−170.

(3) Mantovani, A.; Biswas, S. K.; Galdiero, M. R.; Sica, A.; Locati, M. Macrophage Plasticity and Polarization in Tissue Repair and Remodelling. *J. Pathol.* **2013**, *229* (2), 176−185.

(4) Law, S.; Chaudhuri, S. Mesenchymal Stem Cell and Regenerative Medicine: Regeneration Versus Immunomodulatory Challenges. *Am. J. Stem Cells* **2013**, *2* (1), 22.

DOI: 10.1021/acsami.5b03464
ACS Appl. Mater. Interfaces 2015, 7, 16364−16373

(5) Reya, T.; Morrison, S. J.; Clarke, M. F.; Weissman, I. L. Stem Cells, Cancer, and Cancer Stem Cells. *Nature* **2001**, *414* (6859), 105−111.
(6) Swami, A.; Shi, J.; Gadde, S.; Votruba, A. R.; Kolishetti, N.; Farokhzad, O. C. Nanoparticles for Targeted and Temporally Controlled Drug Delivery. *Multifunctional Nanoparticles for Drug Delivery Applications*; Springer: New York, 2012; pp 9−2910.1007/978-1-4614-2305-8.
(7) Stroncek, J. D.; Reichert, W. M. *Indwelling Neural Implants: Strategies for Contending with the in Vivo Environment*; CRC Press: Boca Raton, FL, USA, 2008.
(8) Makadia, H. K.; Siegel, S. J. Poly Lactic-Co-Glycolic Acid (Plga) as Biodegradable Controlled Drug Delivery Carrier. *Polymers* **2011**, *3* (3), 1377−1397.
(9) Huang, X.; Brazel, C. S. On the Importance and Mechanisms of Burst Release in Matrix-Controlled Drug Delivery Systems. *J. Controlled Release* **2001**, *73* (2), 121−136.
(10) Vallet-Regí, M.; Balas, F.; Colilla, M.; Manzano, M. Drug Confinement and Delivery in Ceramic Implants. *Drug Metab Lett.* **2007**, *1* (1), 37−40.
(11) Yeo, Y.; Park, K. Control of Encapsulation Efficiency and Initial Burst in Polymeric Microparticle Systems. *Arch. Pharmacal Res.* **2004**, *27* (1), 1−12.
(12) Bouissou, C.; Rouse, J.; Price, R.; Van der Walle, C. The Influence of Surfactant on Plga Microsphere Glass Transition and Water Sorption: Remodeling the Surface Morphology to Attenuate the Burst Release. *Pharm. Res.* **2006**, *23* (6), 1295−1305.
(13) Jain, R. A. The Manufacturing Techniques of Various Drug Loaded Biodegradable Poly (Lactide-< I> Co</I>-Glycolide)(Plga) Devices. *Biomaterials* **2000**, *21* (23), 2475−2490.
(14) Ruhe, P. Q.; Hedberg, E. L.; Padron, N. T.; Spauwen, P. H.; Jansen, J. A.; Mikos, A. G. Rhbmp-2 Release from Injectable Poly (Dl-Lactic-Co-Glycolic Acid)/Calcium-Phosphate Cement Composites. *J. Bone Joint Surg. Am.* **2003**, *85* (suppl_3), 75−81.
(15) Danhier, F.; Ansorena, E.; Silva, J. M.; Coco, R.; Le Breton, A.; Préat, V. Plga-Based Nanoparticles: An Overview of Biomedical Applications. *J. Controlled Release* **2012**, *161* (2), 505−522.
(16) Faisant, N.; Akiki, J.; Siepmann, F.; Benoit, J.; Siepmann, J. Effects of the Type of Release Medium on Drug Release from Plga-Based Microparticles: Experiment and Theory. *Int. J. Pharm.* **2006**, *314* (2), 189−197.
(17) Xie, S.; Wang, S.; Zhao, B.; Han, C.; Wang, M.; Zhou, W. Effect of Plga as a Polymeric Emulsifier on Preparation of Hydrophilic Protein-Loaded Solid Lipid Nanoparticles. *Colloids Surf., B* **2008**, *67* (2), 199−204.
(18) Zhou, J.; Guo, D.; Zhang, Y.; Wu, W.; Ran, H.; Wang, Z. Construction and Evaluation of Fe3o4-Based Plga Nanoparticles Carrying Rtpa Used in the Detection of Thrombosis and in Targeted Thrombolysis. *ACS Appl. Mater. Interfaces* **2014**, *6* (8), 5566−5576.
(19) Tasciotti, E.; Liu, X.; Bhavane, R.; Plant, K.; Leonard, A. D.; Price, B. K.; Cheng, M. M.-C.; Decuzzi, P.; Tour, J. M.; Robertson, F.; Ferrari, M. Mesoporous Silicon Particles as a Multistage Delivery System for Imaging and Therapeutic Applications. *Nat. Nanotechnol.* **2008**, *3* (3), 151−157.
(20) Shen, H.; Rodriguez-Aguayo, C.; Xu, R.; Gonzalez-Villasana, V.; Mai, J.; Huang, Y.; Zhang, G.; Guo, X.; Bai, L.; Qin, G.; et al. Enhancing Chemotherapy Response with Sustained Epha2 Silencing Using Multistage Vector Delivery. *Clin. Cancer Res.* **2013**, *19* (7), 1806−1815.
(21) Sun, W.; Puzas, J. E.; Sheu, T. J.; Liu, X.; Fauchet, P. M. Nano- to Microscale Porous Silicon as a Cell Interface for Bone-Tissue Engineering. *Adv. Mater.* **2007**, *19* (7), 921−924.
(22) Chiappini, C.; Tasciotti, E.; Fakhoury, J. R.; Fine, D.; Pullan, L.; Wang, Y. C.; Fu, L.; Liu, X.; Ferrari, M. Tailored Porous Silicon Microparticles: Fabrication and Properties. *ChemPhysChem* **2010**, *11* (5), 1029−1035.
(23) Decuzzi, P.; Godin, B.; Tanaka, T.; Lee, S. Y.; Chiappini, C.; Liu, X.; Ferrari, M. Size and Shape Effects in the Biodistribution of Intravascularly Injected Particles. *J. Controlled Release* **2010**, *141* (3), 320−327.
(24) Martinez, J. O.; Chiappini, C.; Ziemys, A.; Faust, A. M.; Kojic, M.; Liu, X.; Ferrari, M.; Tasciotti, E. Engineering Multi-Stage Nanovectors for Controlled Degradation And tunable Release Kinetics. *Biomaterials* **2013**, *34* (33), 8469−8477.
(25) Fan, D.; De Rosa, E.; Murphy, M. B.; Peng, Y.; Smid, C. A.; Chiappini, C.; Liu, X.; Simmons, P.; Weiner, B. K.; Ferrari, M.; Tasciotti, E. Mesoporous Silicon-Plga Composite Microspheres for the Double Controlled Release of Biomolecules for Orthopedic Tissue Engineering. *Adv. Funct. Mater.* **2012**, *22* (2), 282−293.
(26) De Rosa, E.; Chiappini, C.; Fan, D.; Liu, X.; Ferrari, M.; Tasciotti, E. Agarose Surface Coating Influences Intracellular Accumulation and Enhances Payload Stability of a Nano-Delivery System. *Pharm. Res.* **2011**, *28* (7), 1520−1530.
(27) Fan, D.; De Rosa, E.; Murphy, M. B.; Peng, Y.; Smid, C. A.; Chiappini, C.; Liu, X.; Simmons, P.; Weiner, B. K.; Ferrari, M.; Tasciotti, E. Mesoporous Silicon-Plga Composite Microspheres for the Double Controlled Release of Biomolecules for Orthopedic Tissue Engineering. *Adv. Funct. Mater.* **2012**, *22* (2), 282−293.
(28) De Rosa, E.; Chiappini, C.; Fan, D.; Liu, X.; Ferrari, M.; Tasciotti, E. Agarose Surface Coating Influences Intracellular Accumulation and Enhances Payload Stability of a Nano-Delivery System. *Pharm. Res.* **2011**, *28* (7), 1520−1530.
(29) Minardi, S.; Sandri, M.; Martinez, J. O.; Yazdi, I. K.; Liu, X.; Ferrari, M.; Weiner, B. K.; Tampieri, A.; Tasciotti, E. Multiscale Patterning of a Biomimetic Scaffold Integrated with Composite Microspheres. *Small* **2014**, *10* (19), 3943−3953.
(30) Taraballi, F.; Minardi, S.; Corradetti, B.; Yazdi, I.; Balliano, M.; Van Eps, J.; Allegri, M.; Tasciotti, E. Potential Avoidance of Adverse Analgesic Effects Using a Biologically″ Smart″ Hydrogel Capable of Controlled Bupivacaine Release. *J. Pharm. Sci.* **2014**, *103* (11), 3724−3732.
(31) Park, K.; Mrsny, R. J. *Controlled Drug Delivery: Designing Technologies for the Future*, ed. 1; ACS Symposium Series Vol. *752*; American Chemical Society: Washington, DC, USA, 2000; p 478.
(32) Anderson, J. M.; Shive, M. S. Biodegradation and Biocompatibility of Pla and Plga Microspheres. *Adv. Drug Delivery Rev.* **2012**, *64*, 72−82.
(33) Spiller, K. L.; Anfang, R. R.; Spiller, K. J.; Ng, J.; Nakazawa, K. R.; Daulton, J. W.; Vunjak-Novakovic, G. The Role of Macrophage Phenotype in Vascularization of Tissue Engineering Scaffolds. *Biomaterials* **2014**, *35* (15), 4477−4488.
(34) Taraballi, F.; Minardi, S.; Corradetti, B.; Yazdi, I. K.; Balliano, M. A.; Van Eps, J. L.; Allegri, M.; Tasciotti, E. Potential Avoidance of Adverse Analgesic Effects Using a Biologically "Smart" Hydrogel Capable of Controlled Bupivacaine Release. *J. Pharm. Sci.* **2014**, *103* (11), 3724−3732.
(35) Minardi, S.; Sandri, M.; Martinez, J. O.; Yazdi, I. K.; Liu, X.; Ferrari, M.; Weiner, B. K.; Tampieri, A.; Tasciotti, E. Multiscale Patterning of a Biomimetic Scaffold Integrated with Composite Microspheres. *Small* **2014**, *10* (19), 3943−3953.
(36) Tzur-Balter, A.; Shatsberg, Z.; Beckerman, M.; Segal, E.; Artzi, N. Mechanism of Erosion of Nanostructured Porous Silicon Drug Carriers in Neoplastic Tissues. *Nat. Commun.* **2015**, *6*, 6208.
(37) Langer, R.; Peppas, N. A. Advances in Biomaterials, Drug Delivery, and Bionanotechnology. *AIChE J.* **2003**, *49* (12), 2990−3006.
(38) Lavan, D. A.; McGuire, T.; Langer, R. Small-Scale Systems for in Vivo Drug Delivery. *Nat. Biotechnol.* **2003**, *21* (10), 1184−1191.
(39) Epstein, N. E. Complications Due to the Use of Bmp/Infuse in Spine Surgery: The Evidence Continues to Mount. *Surg. Neurol. Int.* **2013**, *4* (6 (Suppl 5)), 343.
(40) Epstein, N. E. Pros, Cons, and Costs of Infuse in Spinal Surgery. *Surg. Neurol. Int.* **2011**, *2* (1), 10.
(41) Carragee, E. J.; Chu, G.; Rohatgi, R.; Hurwitz, E. L.; Weiner, B. K.; Yoon, S. T.; Comer, G.; Kopjar, B. Cancer Risk after Use of Recombinant Bone Morphogenetic Protein-2 for Spinal Arthrodesis. *J. Bone Joint Surg. Am.* **2013**, *95* (17), 1537−1545.
(42) Anselmo, A. C.; Mitragotri, S. An Overview of Clinical and Commercial Impact of Drug Delivery Systems. *J. Controlled Release* **2014**, *190*, 15−28.

DOI: 10.1021/acsami.5b03464
ACS Appl. Mater. Interfaces 2015, 7, 16364−16373